Modulating the Second Peak of a First-Passage-Time Distribution by Scanning the Destination of a Directed Shortcut (Fixed N=100, K=6; Analytic inversion, flux validation, and Monte Carlo)

1 Introduction and objective

Under the start/target configuration used in the main manuscript, I fix $(N, K) = (100, 6)$ and vary only the shortcut destination dst. I aim to:

- quantify how the peak timings and the relative second-peak prominence (e.g., $R = A(t_2)/A(t_1)$) change with dst;
- estimate, among trajectories whose absorption times fall near the second peak, the conditional shortcut-crossing probabilities.

2 Setup

2.1 Model and fixed parameters

- Nodes are labeled $1, \ldots, N$ with $N = 100$.
- Initial node: $n_0 = 1$.
- Absorbing target: target $= N/2 = 50$ (strict first passage; $\rho = 1$).
- Ring connectivity: $K = 6$ neighbors $(\pm 1, \pm 2, \pm 3)$.
- A single directed shortcut from src to dst, where dst is scanned.
- I compare two choices of shortcut source:
  - Case A: src $= n_0 + 5 = 6$.
  - Case B: src $= n_0 = 1$.

3 Main conclusions

- Scanning only dst (with $N = 100$, $K = 6$, $n_0 = 1$, target $= 50$ fixed) strongly modulates the peak timings and the *relative* prominence of the second peak (captured by the ratio $R = A(t_2)/A(t_1)$). In the late-second-peak family, the absolute second-peak height $A(t_2)$ varies only weakly across dst, except for special near-target cases.
- A deterministic flux/master-equation scan reproduces the bimodal dst sets and matches the AW inversion over $t \leq 2000$ (max absolute error $\sim 10^{-13}$ on representative cases), indicating the bimodality is not a numerical artifact.
- For late-second-peak cases, the conditional shortcut-usage probability is more cleanly organized by the peak ratio R (excluding the special dst = target point): empirically $P(C \geq 1 \mid T \in W)$ tends to decrease as R increases. $A(t_2)$ shows a positive association with $P(C \geq 1 \mid T \in W)$, but its dynamic range is comparatively small in the late family.
- Case B (src = 1) additionally exhibits an early-t_2 family when dst is close to the target, due to a two-step absorbing path; in these cases, conditional on $T \in W$ shortcut usage is typically near-deterministic ($P(C \geq 1 \mid T \in W) \approx 1$).

- If I focus on Case A, the first/second peaks are typically smoother late-time features (as opposed to the near-delta early peaks in Case B), and the conditional crossing fractions are correspondingly more informative and stable across dst (with visibly nontrivial mass at $C = 0$, $C = 1$, and sometimes $C \geq 2$).

4 Methods

4.1 Second-peak identification and MC conditioning

- I use the peak-selection rule from the caption of Fig. 3 in the manuscript: local maxima with $A(t) > 10^{-7}$; the second peak must reach at least 1% of the global maximum.
- $A(t)$ is a discrete-time first-passage-time probability mass function, so the plotted polyline is not expected to be smooth.
- Denote the first two peaks as (t_1, t_2). I define a symmetric window around the second peak via

$$\Delta = \max\{1, \lfloor 0.05\,(t_2 - t_1)\rfloor\}, \qquad W = [t_2 - \Delta,\ t_2 + \Delta].$$

  In MC I retain only trajectories with absorption time $T \in W$ and record their shortcut crossing count C (0, 1, or ≥ 2).

4.2 Estimands and Monte Carlo estimators

Each trajectory yields a pair (T, C):

- T: first-passage absorption time (the number of steps until first hitting target).
- C: the shortcut traversal count, i.e., the number of times the edge src $\to$ dst is used.

The main conditional quantities of interest are

$$P(C = 0 \mid T \in W), \qquad P(C \geq 1 \mid T \in W) = 1 - P(C = 0 \mid T \in W),$$

and additionally $P(C = 1 \mid T \in W)$ and $P(C \geq 2 \mid T \in W)$. If $n = |\{i : T_i \in W\}|$ and $k_0 = |\{i : T_i \in W,\ C_i = 0\}|$, then

$$\widehat{P}(C = 0 \mid T \in W) = k_0/n, \qquad \widehat{P}(C \geq 1 \mid T \in W) = 1 - k_0/n.$$

For uncertainty visualization I use Wilson 95% confidence intervals for the Bernoulli event $\{C \geq 1\}$ (computed by the plotting script). I also report the window hit rate n/N_{walkers}; if n is too small (e.g., $< 10^3$), the estimated fractions have substantial sampling error.

5 Deterministic validation (flux/master equation)

5.1 Method (time-domain flux / master equation)

Treat target as absorbing, propagate the transient mass $p_t(i)$ deterministically, and read off the FPT pmf as the flux into the target:

$$f(t+1) = p_{t+1}(\text{target}), \qquad p_{t+1}(j) = \sum_i p_t(i) P(i \to j),\ j \neq \text{target}.$$

Implementation uses a directed edge list $(\text{src}, \text{dst}, w)$ with $w = 1/\deg(\text{src})$ for a sparse $O(E)$ update per step (no dense $(N \times N)$ matrix). This provides a deterministic check that bimodality is not a Monte Carlo artifact and that the AW inversion agrees with a time-domain baseline.

5.2 Bimodality criteria (Fig. 3 + separation)

- Fig. 3-caption style: strict local maxima with $f(t) > 10^{-7}$; the second peak must be at least 1% of the global maximum peak height.
- Separation/robust filter: additionally require the two peaks to be separated by at least $2K = 12$ to exclude early "micro-peak clusters".
- Valley-depth diagnostic: with $h_{\min} = \min\{f(t_1), f(t_2)\}$,

$$V = \frac{\min_{t_1<t<t_2} f(t)}{h_{\min}}.$$

  $V \approx 1$ means the valley between the two peaks is shallow.

5.3 Scan results (Case A: src $= 6$)

With $(N, K, n_0, \text{target}) = (100, 6, 1, 50)$ fixed and scanning dst:

- Fig. 3 criterion finds 15 bimodal destinations dst $\in \{43, \ldots, 57\}$ (including the special dst $=$ target $= 50$).
- The separation/robust filter keeps 14: dst $\in \{43, \ldots, 49, 51, \ldots, 57\}$.

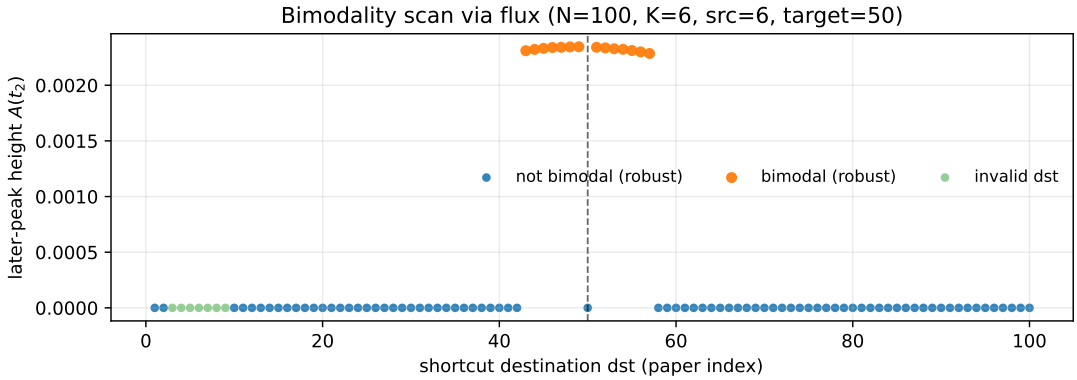


Figure 1: Case A: flux/master-equation scan over dst and the late-peak height $A(t_2) = f(t_2)$ (dashed line: dst $=$ target $= 50$).

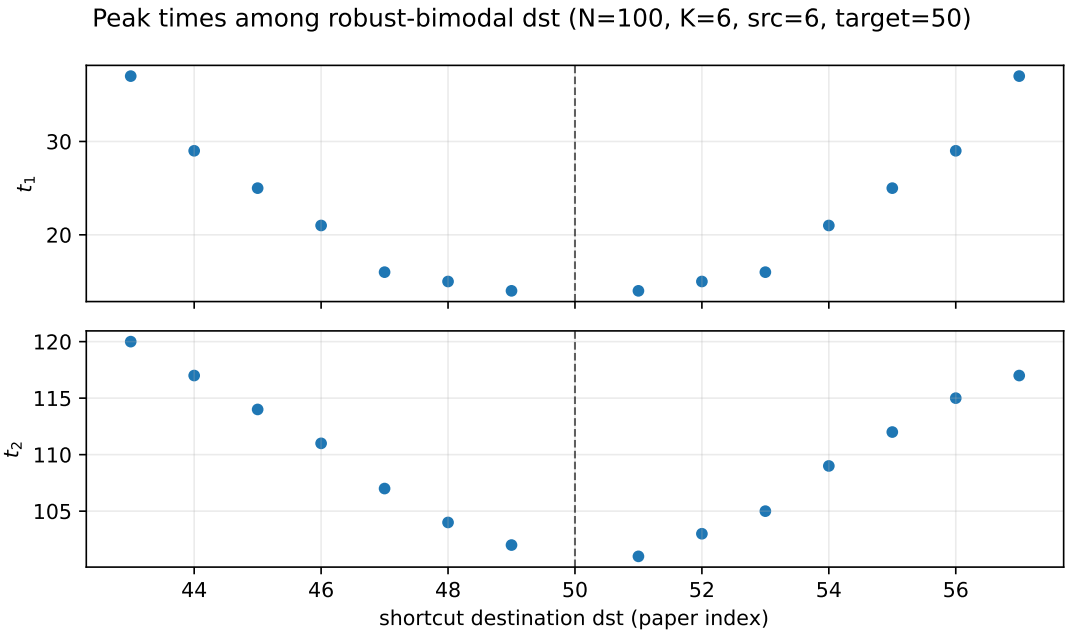


Figure 2: Case A: peak times t_1, t_2 among robust bimodal destinations.

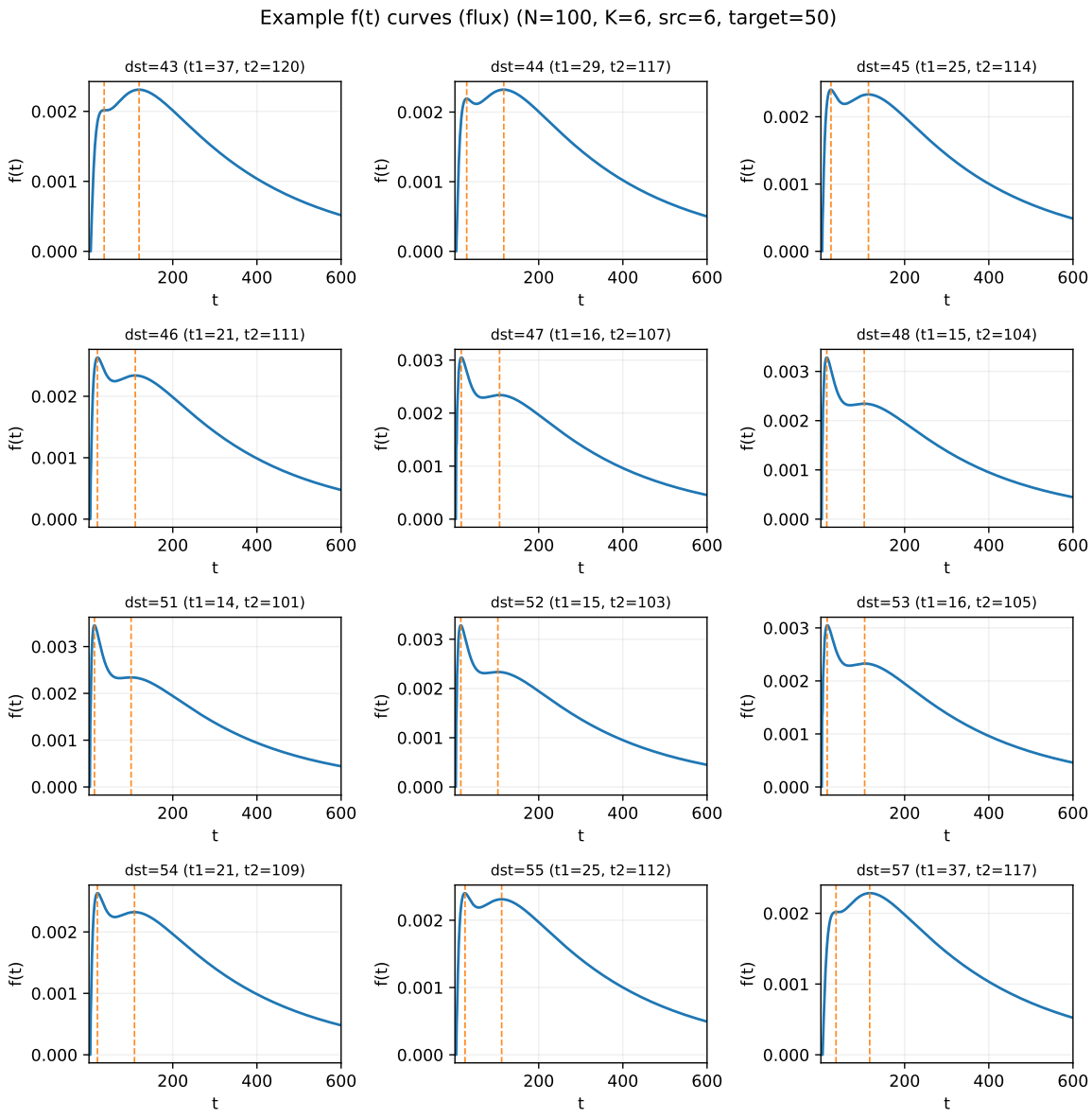


Figure 3: Case A: representative robust bimodal pmfs $f(t)$ (flux), with t_1, t_2 marked.

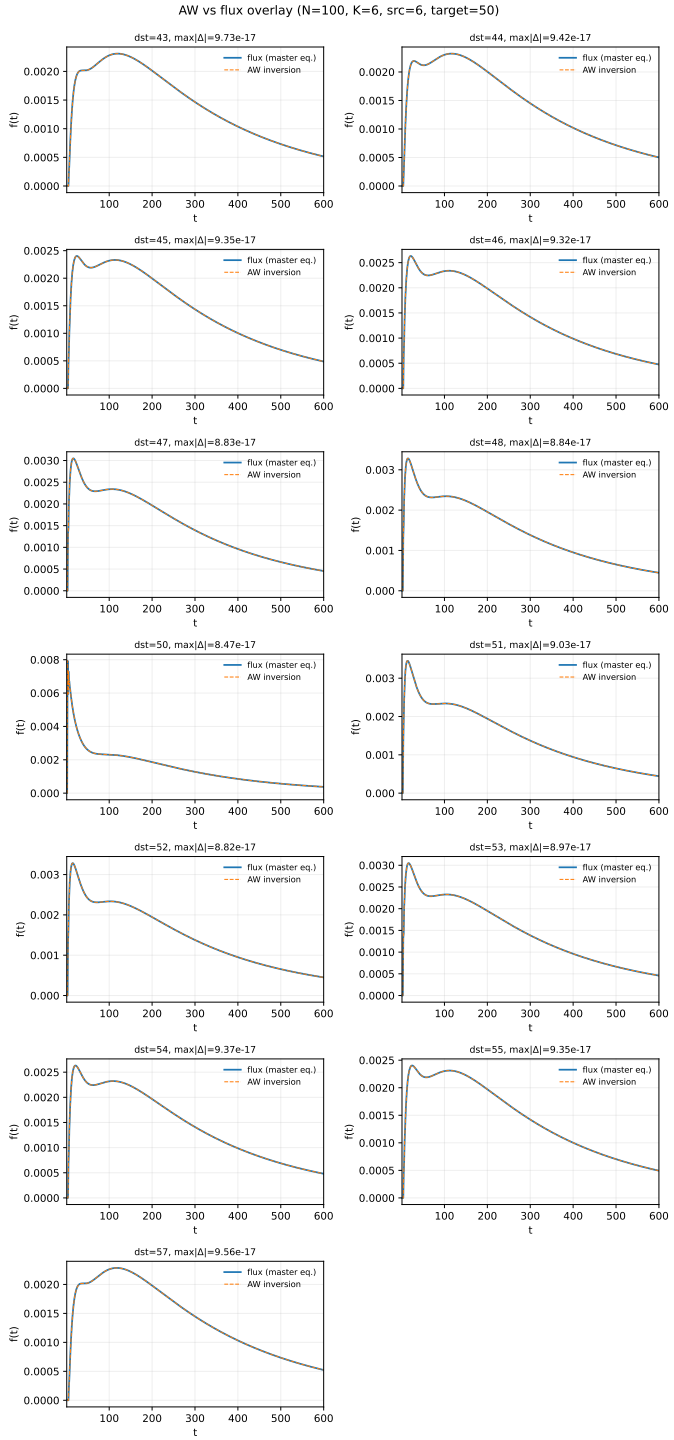


Figure 4: Case A: AW inversion vs. flux $f(t)$ overlays (max error $\sim 10^{-13}$).

dst	t_1	t_2	$t_2 - t_1$	$A(t_1)$	$A(t_2)$	V
43	37	120	83	0.00201691	0.00231041	1.000
44	29	117	88	0.00219366	0.00232199	0.965
45	25	114	89	0.00240315	0.00233158	0.940
46	21	111	90	0.00263207	0.00233914	0.960
47	16	107	91	0.00304909	0.00234085	0.979
48	15	104	89	0.00328311	0.00234431	0.987
49	14	102	88	0.00345483	0.00234556	0.992
51	14	101	87	0.00345483	0.0023412	0.993
52	15	103	88	0.00328311	0.00233559	0.989
53	16	105	89	0.00304909	0.00232787	0.982
54	21	109	88	0.00263207	0.00232303	0.965
55	25	112	87	0.00240315	0.00231205	0.947
56	29	115	86	0.00219365	0.00229944	0.965
57	37	117	80	0.0020168	0.00228525	0.999

5.4 Scan results (Case B: src = 1)

- Fig. 3 criterion finds 18 bimodal destinations, but many are early-time peak clusters (separation $< 2K$).
- After the separation/robust filter, 7 remain as typical "late second peak" cases: dst $\in \{36, 37, 38, 39, 62, 63, 64\}$.

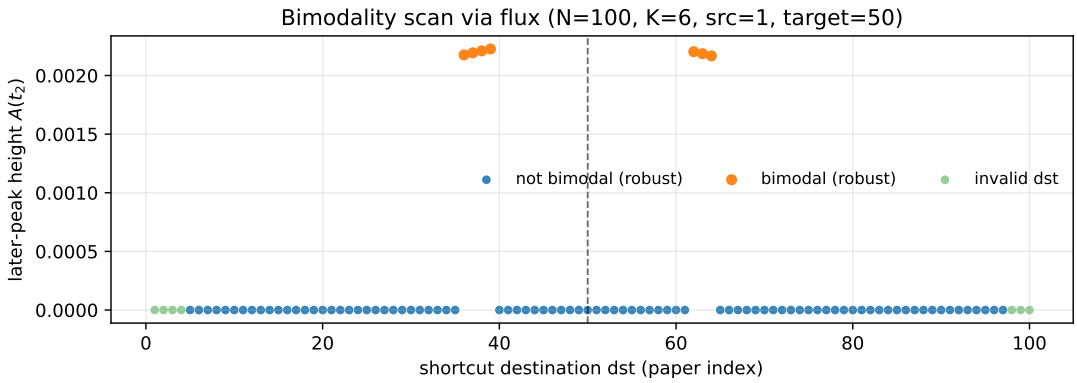


Figure 5: Case B: flux scan over dst and the late-peak height $A(t_2) = f(t_2)$ (robust cases highlighted).

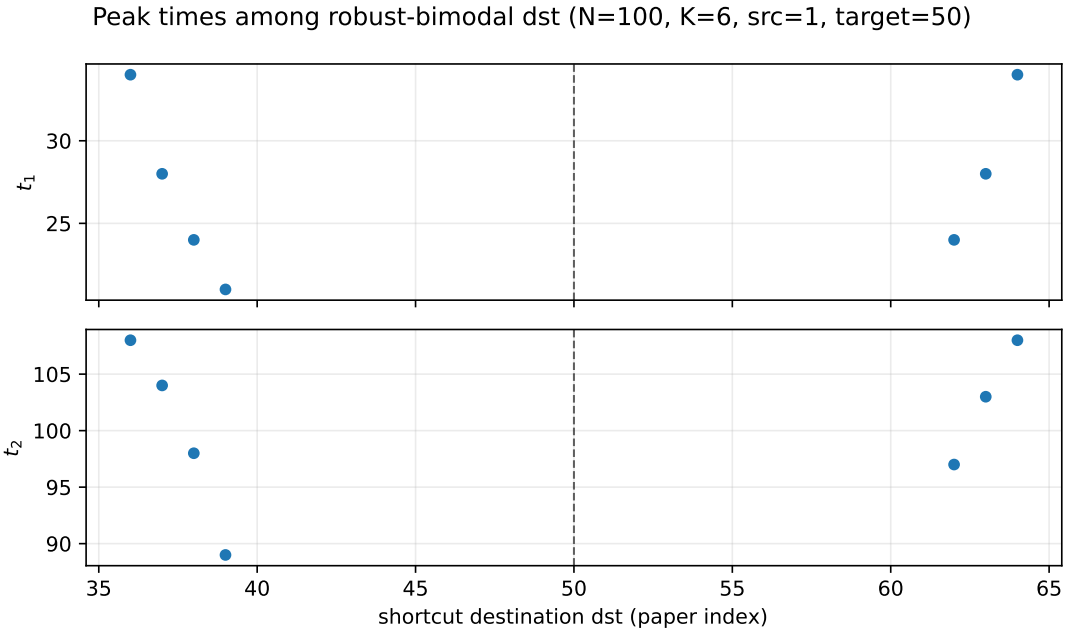


Figure 6: Case B: peak times t_1, t_2 among robust bimodal destinations.

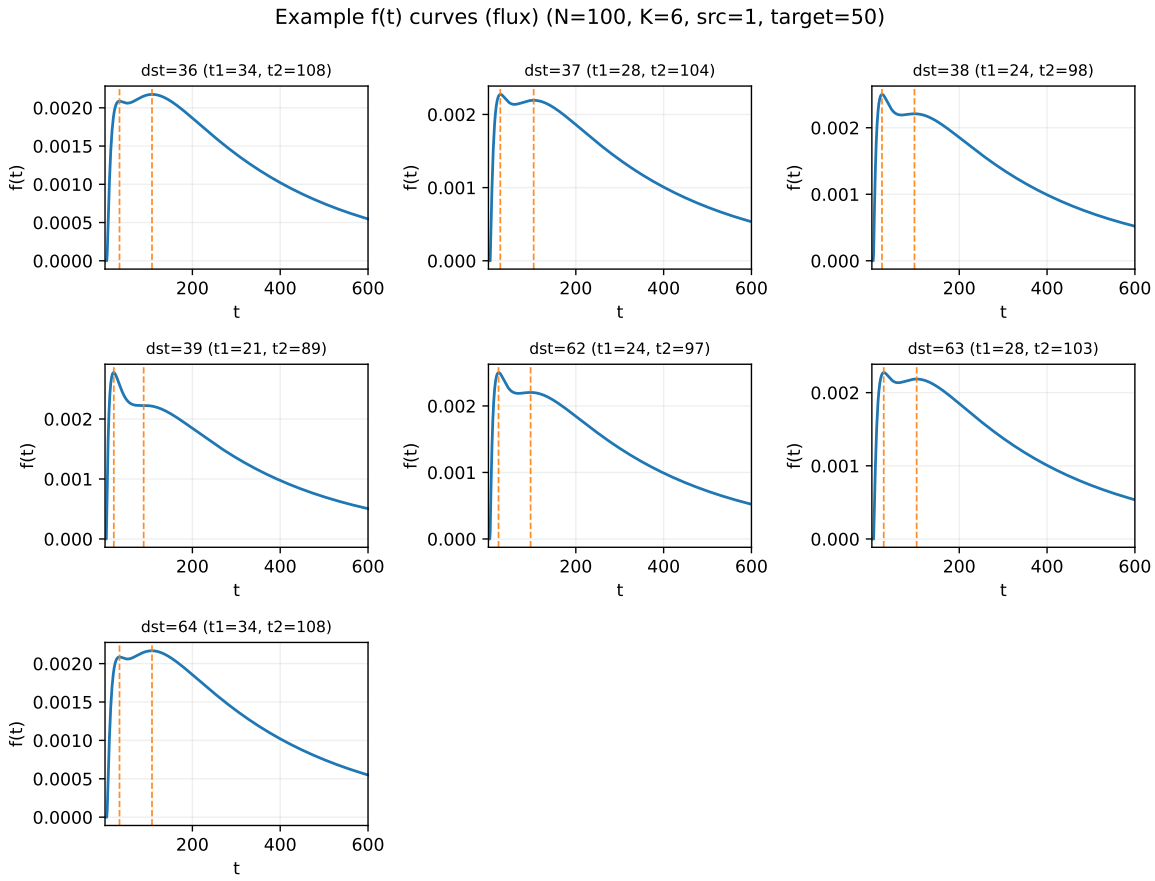


Figure 7: Case B: representative robust bimodal pmfs $f(t)$ (flux), with t_1, t_2 marked.

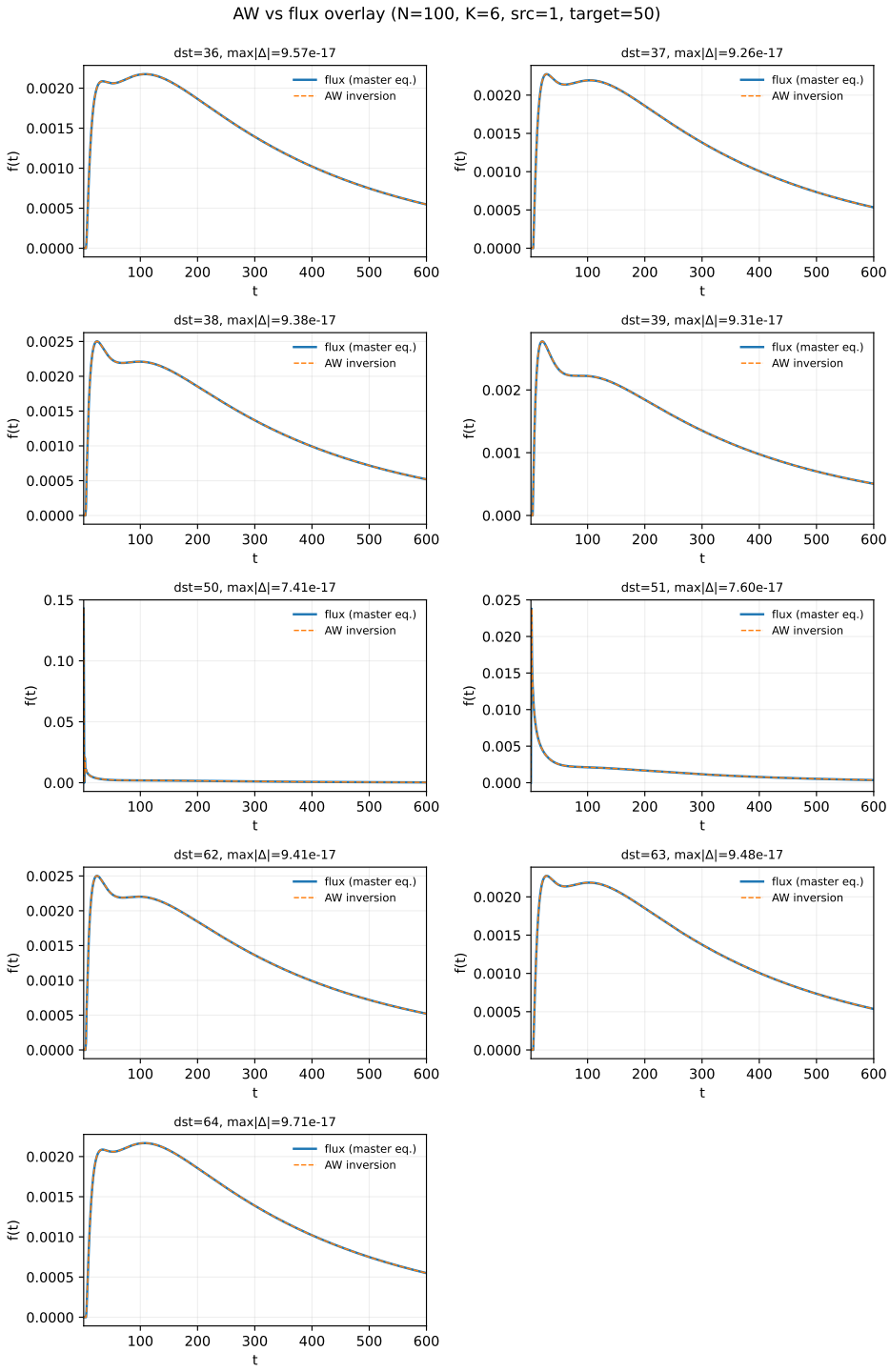


Figure 8: Case B: AW inversion vs. flux $f(t)$ overlays (max error $\sim 10^{-13}$).

dst	t_1	t_2	$t_2 - t_1$	$A(t_1)$	$A(t_2)$	V
36	34	108	74	0.00208676	0.00217576	0.988
37	28	104	76	0.00227434	0.0021934	0.975
38	24	98	74	0.00250164	0.00220997	0.992
39	21	89	68	0.00277427	0.00222632	1.000
62	24	97	73	0.00250164	0.00220303	0.993
63	28	103	75	0.00227434	0.00218569	0.977
64	34	108	74	0.00208671	0.00216745	0.987

5.5 Reproducibility (flux scan)

- Case A: `python3 code/bimodality_flux_scan.py --sc-src 6 --aw-check`
- Case B: `python3 code/bimodality_flux_scan.py --sc-src 1 --aw-check`

6 Results: Case A (src = 6)

6.1 MC scan scope

- Parameter set: $N = 100,\ K = 6,\ n_0 = 1,\ \text{target} = 50,\ \text{src} = 6$.
- Number of dst values satisfying the bimodality criterion (Fig. 3 rule): 15, spanning 43–57.
- Special case: dst = target = 50 connects the shortcut directly to the absorber, yielding an early window and $P(C \geq 1) \approx 1$.

6.2 Analytic second-peak height vs. dst

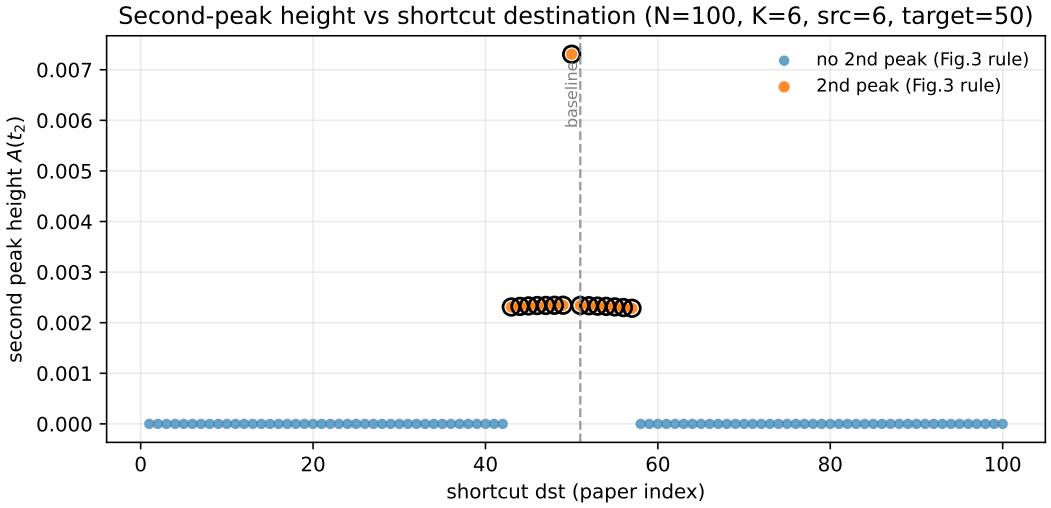


Figure 9: Analytic (Abate–Whitt inversion) second-peak height $A(t_2)$ as a function of shortcut destination dst.

6.3 Peak times (t1, t2) among bimodal cases

6.4 Mechanism: late second peak in Case A

- In Case A, src $\neq n_0$: a trajectory must first reach src = 6 before it can use the shortcut, so shortcut-induced effects typically manifest on later time scales.
- Bimodality can be interpreted as a mixture of two trajectory classes: those that reach src and utilize the shortcut relatively early (contributing to the earlier peak at t_1), and those that do not effectively utilize the shortcut until much later (contributing to the later peak at $t_2 \sim O(N)$).

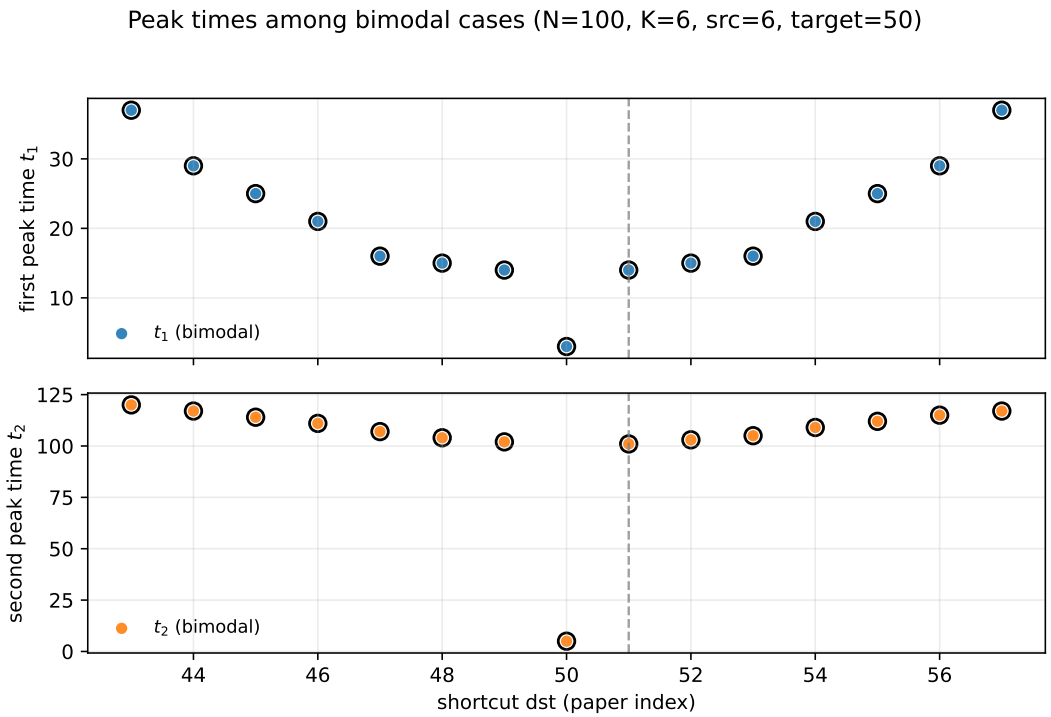


Figure 10: Peak locations t_1 and t_2 as functions of dst, restricted to cases satisfying the bimodality criterion.

- The special point dst = target connects directly to the absorbing state and produces an atypically early peak structure; it should be considered separately from typical late-second-peak behavior.

6.5 Representative FPT curves and second-peak windows

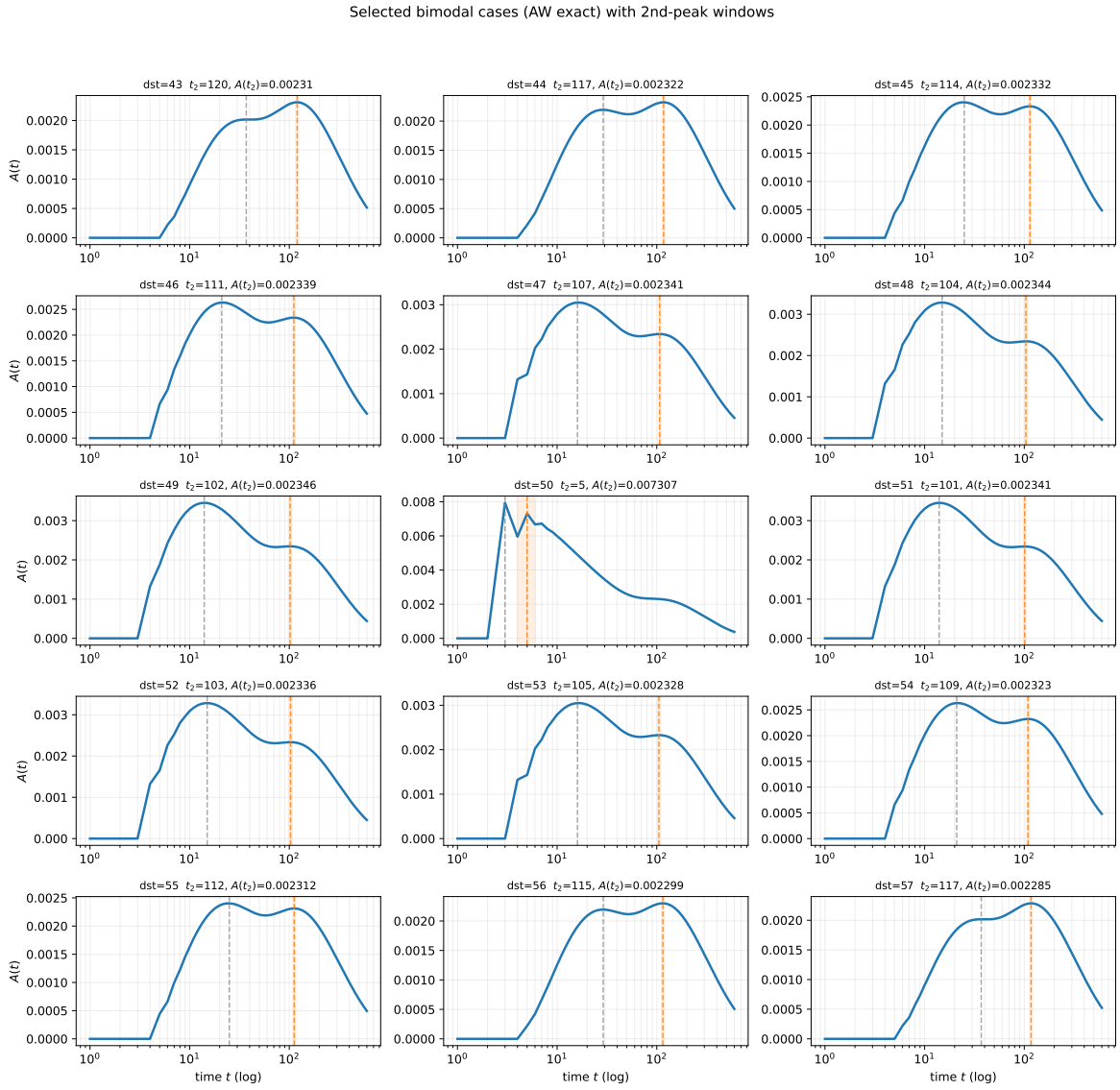


Figure 11: Analytic $A(t)$ (Abate–Whitt inversion) for all dst satisfying the bimodality criterion. Orange shading indicates the second-peak window $W = [t_2 - \Delta, t_2 + \Delta]$.

6.6 MC shortcut-crossing fractions within the second-peak window

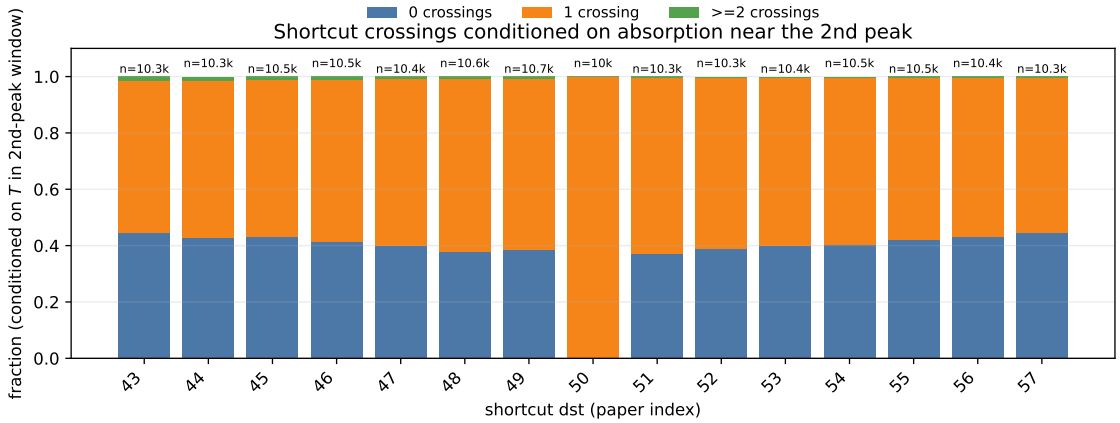


Figure 12: For each dst, conditional on $T \in W$, I estimate the fractions of trajectories with $C = 0$, $C = 1$, and $C \geq 2$ (stacked bars). The label atop each bar reports the window sample size n.

6.7 Relationship between second-peak prominence and shortcut usage

Define the peak-height ratio $R = A(t_2)/A(t_1)$. I examine how $P(C \geq 1 \mid T \in W)$ varies with R and with the absolute height $A(t_2)$.

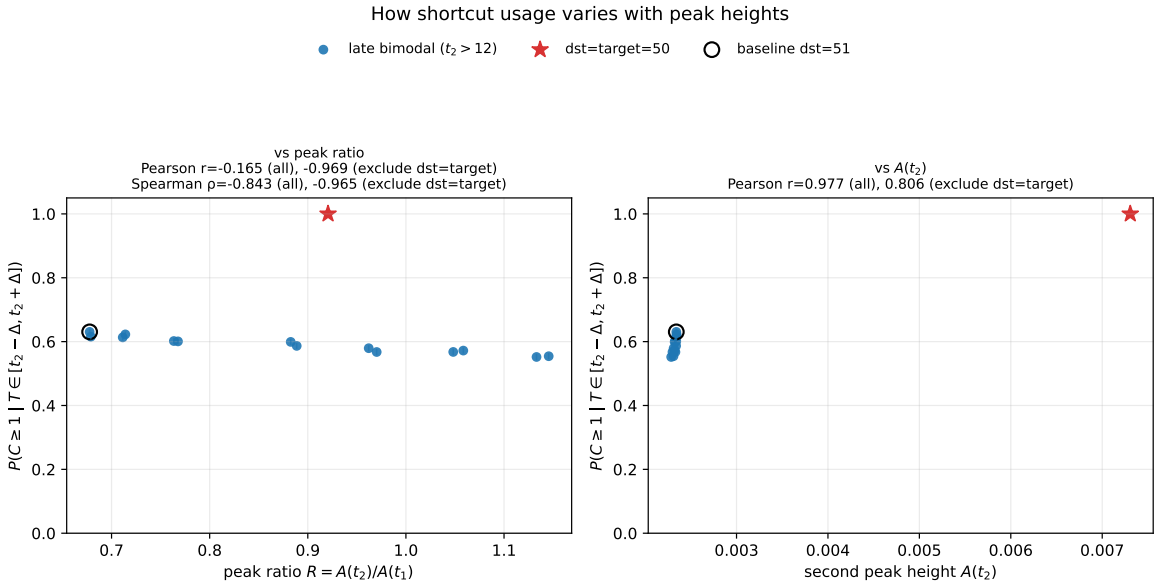


Figure 13: Left: $P(C \geq 1 \mid T \in W)$ vs. R; right: $P(C \geq 1 \mid T \in W)$ vs. $A(t_2)$. Error bars are Wilson 95% confidence intervals. Colors indicate early/late (early defined by $t_2 \leq 2K$; Case A is almost entirely late). The red star denotes the special case dst = target.

6.7.1 Correlation summary (computed by script)

- Pearson $r(R,\ P(C \geq 1))$: -0.165 (all), -0.969 (excluding dst = target).
- Spearman $\rho(R,\ P(C \geq 1))$: -0.843 (all), -0.965 (excluding dst = target).
- Pearson $r(A(t_2),\ P(C \geq 1))$: 0.977 (all), 0.806 (excluding dst = target).
- (Equivalently) Pearson $r(A(t_2),\ P(C = 0))$: -0.977 (all), -0.806 (excluding dst = target).

- (Late-only: $t_2 > 12$) Pearson $r(A(t_2),\ P(C \geq 1))$: 0.806; Pearson $r(R,\ P(C \geq 1))$: -0.969.

6.7.2 Key takeaways (Case A)

- **Predominantly late bimodality:** aside from dst = target, bimodal cases in Case A are mainly late-second-peak instances (large t_2).
- **Nontrivial zero-crossing mass:** even conditional on $T \in W$, a substantial fraction of trajectories have $C = 0$, indicating the second peak reflects a slower subpopulation rather than paths that almost surely traverse the shortcut.
- **Monotone trend with $A(t_2)$:** larger $A(t_2)$ is associated with larger $P(C \geq 1 \mid T \in W)$ (equivalently, smaller $P(C = 0 \mid T \in W)$).
- **Special case** dst = target**:** the second peak occurs very early and $P(C \geq 1 \mid T \in W) \approx 1$, so this point should be discussed separately.

6.8 Summary table

dst	t_1	t_2	Δ	R	$A(t_1)$	$A(t_2)$	$P(C=0)$	$P(C \geq 1)$
43	37	120	4	1.146	0.0020160646	0.00231041	0.446	0.554
44	29	117	4	1.059	0.0021926251	0.00232199	0.428	0.572
45	25	114	4	0.970	0.0024036907	0.00233158	0.432	0.568
46	21	111	4	0.889	0.0026312025	0.00233914	0.413	0.587
47	16	107	4	0.768	0.0030482422	0.00234085	0.399	0.601
48	15	104	4	0.714	0.0032836275	0.00234431	0.377	0.623
49	14	102	4	0.679	0.0034545803	0.00234556	0.384	0.616
50	3	5	1	0.921	0.0079321716	0.00730663	0.000	1.000
51	14	101	4	0.678	0.0034530973	0.0023412	0.369	0.631
52	15	103	4	0.711	0.0032842321	0.00233559	0.387	0.613
53	16	105	4	0.763	0.0030519913	0.00232787	0.398	0.602
54	21	109	4	0.883	0.0026314043	0.00232303	0.401	0.599
55	25	112	4	0.962	0.0024021309	0.00231205	0.421	0.579
56	29	115	4	1.048	0.0021939313	0.00229944	0.432	0.568
57	37	117	4	1.133	0.0020169903	0.00228525	0.448	0.552

7 Results: Case B (src = 1)

7.1 MC scan scope

- Parameter set: $N = 100,\ K = 6,\ n_0 = 1,\ \text{target} = 50,\ \text{src} = 1$.
- Number of dst values satisfying the bimodality criterion (Fig. 3 rule): 18, spanning 36–64.
- Special case: dst = target = 50 connects the shortcut directly to the absorber, yielding an early window and $P(C \geq 1) \approx 1$.

7.2 Analytic second-peak height vs. dst

7.3 Peak times (t1, t2) among bimodal cases

7.4 Why can "second peaks" occur at very early times in Case B?

- When src = n_0, the shortcut is available immediately: at step 1 the walker uses the shortcut $n_0 \to$ dst with probability $1/(K+1) = 1/7$.
- If dst is within one ring step of the target (i.e., dst $\in \{\text{target} \pm 1, \pm 2, \pm 3\}$ for $K = 6$), there exist extremely short absorbing paths

$$n_0 \xrightarrow{\text{shortcut}} \text{dst} \xrightarrow{\text{ring}} \text{target},$$

which create a large absorption probability already at $t = 2$ and hence produce an early peak structure (and these early peaks are almost entirely composed of trajectories that traverse the shortcut).

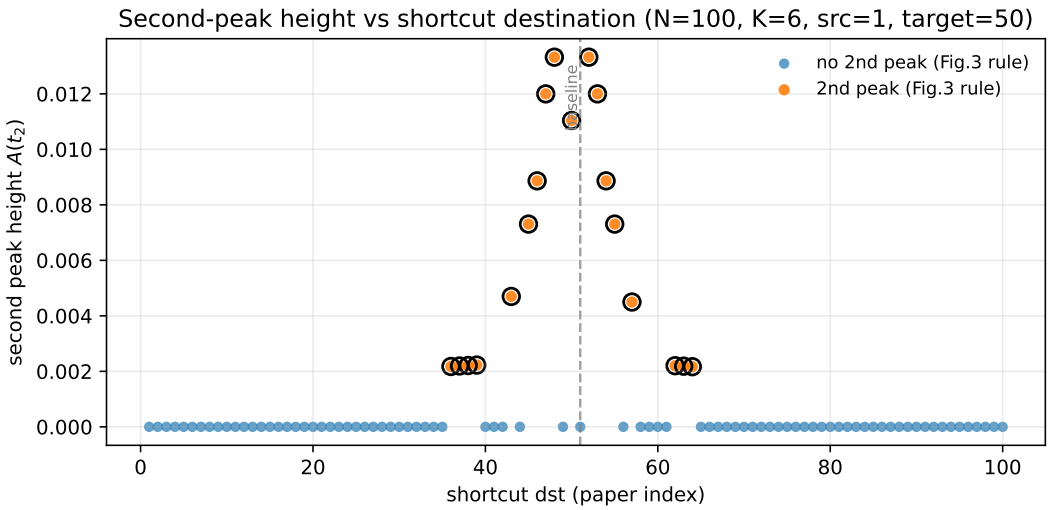


Figure 14: Analytic (Abate–Whitt inversion) second-peak height $A(t_2)$ as a function of shortcut destination dst.

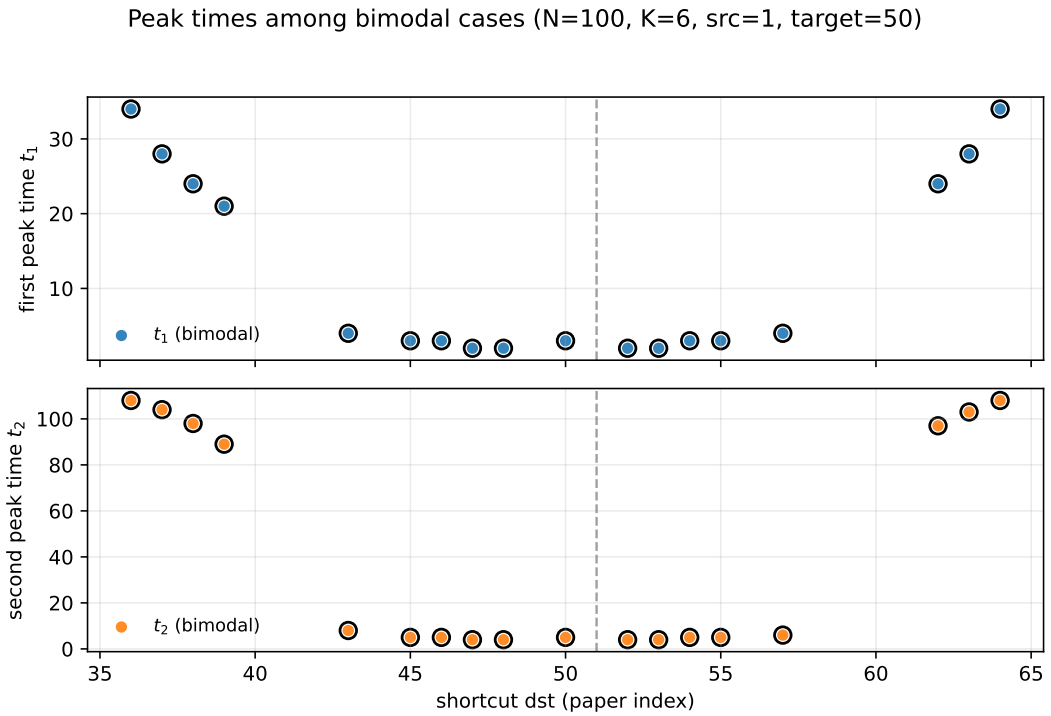


Figure 15: Peak locations t_1 and t_2 as functions of dst, restricted to cases satisfying the bimodality criterion.

- These early peaks are not numerical artifacts: for representative early-t_2 cases (e.g., dst = 47), comparison to exact master-equation propagation shows that Abate–Whitt inversion matches the exact values over the first 200 steps with maximum error $\sim 10^{-14}$ and agrees in both peak locations and heights.

7.5 Mechanism: late second peak in Case B

- Case B also exhibits late-second-peak instances: when the shortcut sends the walker far from the target, early shortcut usage can delay absorption.
- This separates trajectories into two classes: those that do not use the shortcut early (or are not substantially displaced by it), contributing to the earlier peak at t_1, and those that use the shortcut early and are pushed away from the target, contributing to the later peak at t_2.
- In these late-t_2 cases, conditional on $T \in W$ I typically observe $P(C \geq 1 \mid T \in W) \approx 0.63$–$0.72$, leaving a visible zero-crossing fraction.

7.6 Representative FPT curves and second-peak windows

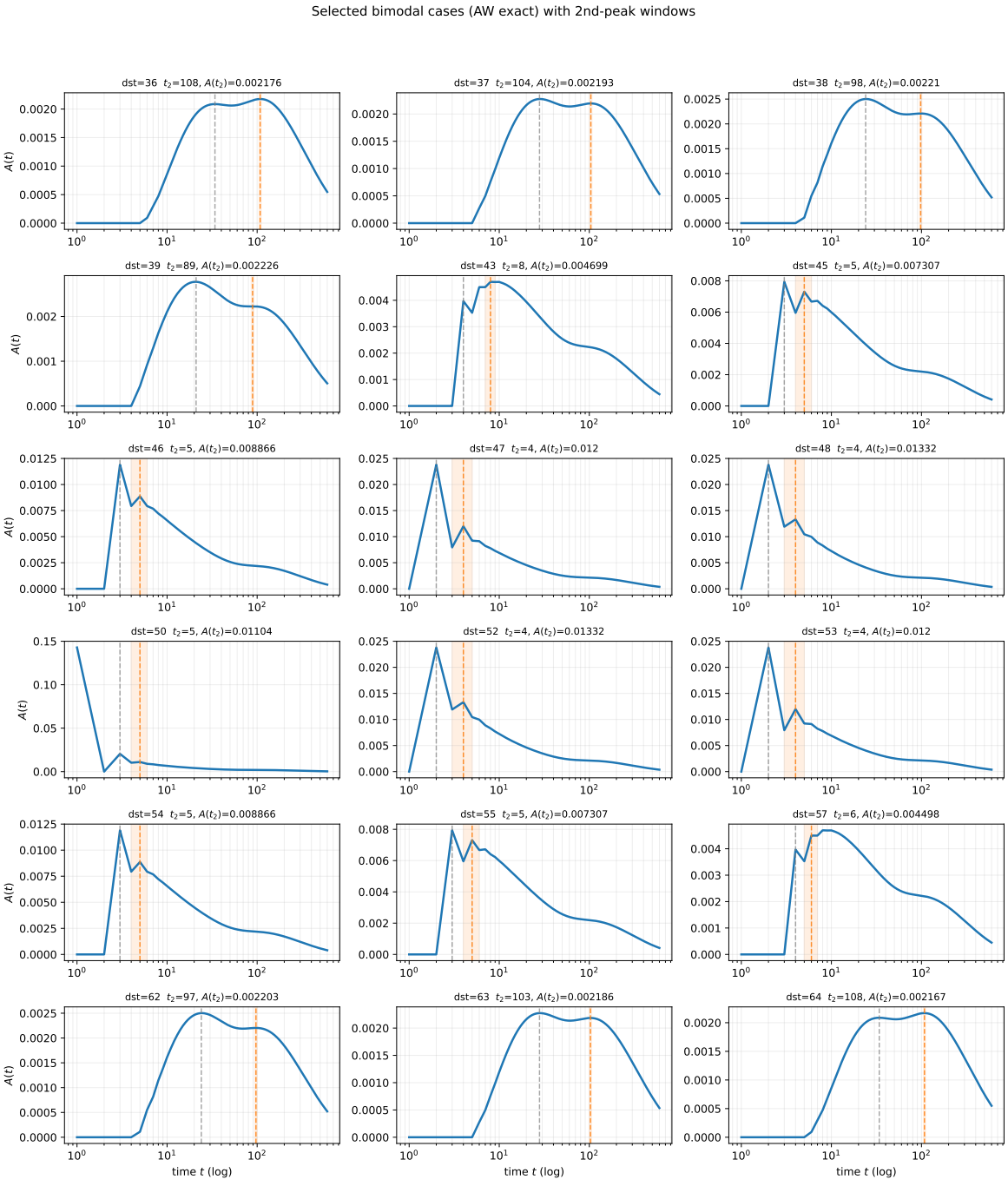


Figure 16: Analytic $A(t)$ (Abate–Whitt inversion) for all dst satisfying the bimodality criterion. Orange shading indicates the second-peak window $W = [t_2 - \Delta, t_2 + \Delta]$.

7.7 MC shortcut-crossing fractions within the second-peak window

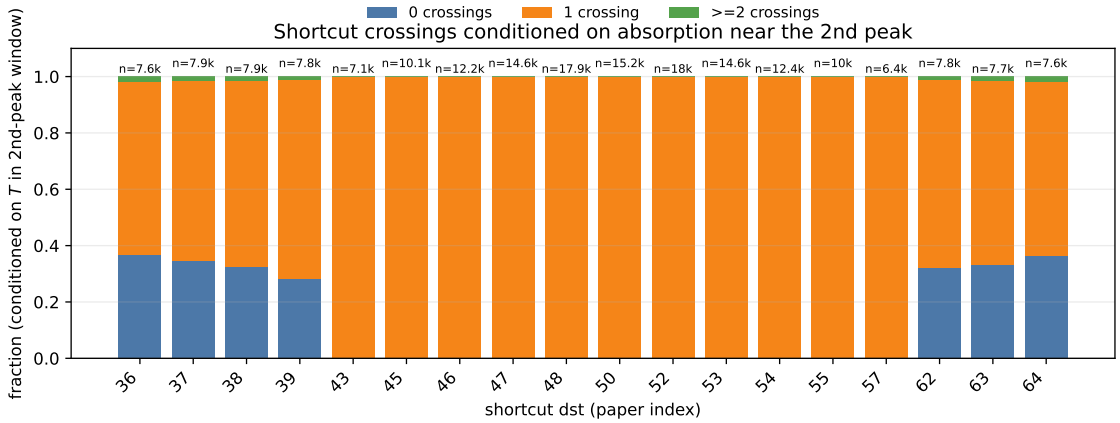


Figure 17: For each dst, conditional on $T \in W$, I estimate the fractions of trajectories with $C = 0$, $C = 1$, and $C \geq 2$ (stacked bars). The label atop each bar reports the window sample size n.

7.8 Relationship between second-peak prominence and shortcut usage

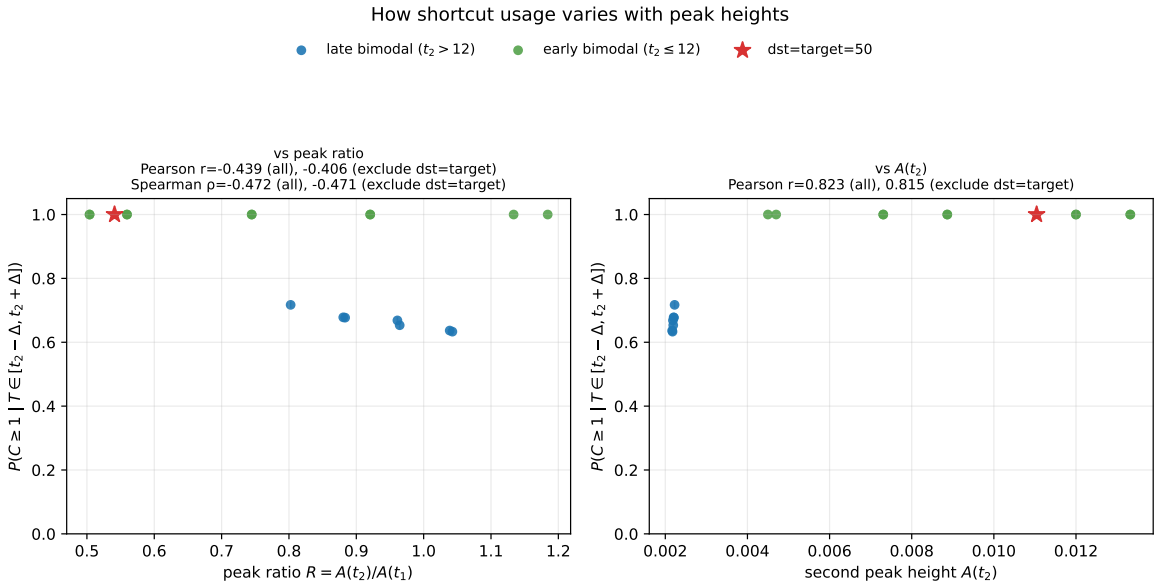


Figure 18: Left: $P(C \geq 1 \mid T \in W)$ vs. R; right: $P(C \geq 1 \mid T \in W)$ vs. $A(t_2)$. Error bars are Wilson 95% confidence intervals. Colors indicate early/late (early defined by $t_2 \leq 2K$). The red star denotes the special case dst = target.

7.8.1 Correlation summary (computed by script)

- Pearson $r(R,\ P(C \geq 1))$: -0.439 (all), -0.406 (excluding dst = target).
- Spearman $\rho(R,\ P(C \geq 1))$: -0.472 (all), -0.471 (excluding dst = target).
- Pearson $r(A(t_2),\ P(C \geq 1))$: 0.823 (all), 0.815 (excluding dst = target).
- (Equivalently) Pearson $r(A(t_2),\ P(C = 0))$: -0.823 (all), -0.815 (excluding dst = target).
- (Late-only: $t_2 > 12$) Pearson $r(A(t_2),\ P(C \geq 1))$: 0.938; Pearson $r(R,\ P(C \geq 1))$: -0.973.

7.8.2 Key takeaways (Case B)

- **Two mechanisms:** with src $= n_0$, bimodal cases typically split into an early-t_2 class (e.g., $t_2 \leq 8$) and a late-t_2 class (e.g., $t_2 \approx 90$–110).
- **Early-t_2 cases:** conditional on $T \in W$, trajectories almost surely traverse the shortcut, so $P(C \geq 1 \mid T \in W) \approx 1$ (and typically $C = 1$).
- **Late-t_2 cases:** conditional on $T \in W$, a substantial zero-crossing fraction remains (roughly 0.28–0.37 in this scan).
- **Trend with $A(t_2)$:** overall, smaller $A(t_2)$ is associated with smaller $P(C \geq 1 \mid T \in W)$ (equivalently, larger $P(C = 0 \mid T \in W)$). Thus the statement "a lower second peak implies a higher shortcut-usage fraction" is not supported here; the observed trend is the opposite.
- **Special case** dst = target**:** the shortcut points directly to the absorber, producing an early window and $P(C \geq 1 \mid T \in W) \approx 1$, and should be separated from the late-second-peak mechanism.

7.9 Summary table

dst	t_1	t_2	Δ	R	$A(t_1)$	$A(t_2)$	$P(C=0)$	$P(C\geq 1)$
36	34	108	3	1.043	0.0020860594	0.00217576	0.367	0.633
37	28	104	3	0.964	0.0022753112	0.0021934	0.347	0.653
38	24	98	3	0.883	0.0025027973	0.00220997	0.323	0.677
39	21	89	3	0.802	0.0027759601	0.00222632	0.283	0.717
43	4	8	1	1.184	0.0039697399	0.00469917	0.000	1.000
45	3	5	1	0.921	0.0079321716	0.00730663	0.000	1.000
46	3	5	1	0.745	0.011900107	0.00886558	0.000	1.000
47	2	4	1	0.504	0.023807937	0.0119992	0.000	1.000
48	2	4	1	0.560	0.023789286	0.013322	0.000	1.000
50	3	5	1	0.541	0.020408317	0.0110409	0.000	1.000
52	2	4	1	0.560	0.023789286	0.013322	0.000	1.000
53	2	4	1	0.504	0.023807937	0.0119992	0.000	1.000
54	3	5	1	0.745	0.011900107	0.00886558	0.000	1.000
55	3	5	1	0.921	0.0079321716	0.00730663	0.000	1.000
57	4	6	1	1.134	0.003966843	0.0044984	0.000	1.000
62	24	97	3	0.881	0.0025011691	0.00220303	0.322	0.678
63	28	103	3	0.961	0.0022743913	0.00218569	0.332	0.668
64	34	108	3	1.039	0.0020860924	0.00216745	0.363	0.637

Reproducibility: flux scan (deterministic):

Case A: `python3 code/bimodality_flux_scan.py --sc-src 6 --aw-check`

Case B: `python3 code/bimodality_flux_scan.py --sc-src 1 --aw-check`

dst scan + MC:

Case A: `python3 code/dst_shortcut_usage_mc.py --sc-src 6 --mc-all-bimodal`

Case B: `python3 code/dst_shortcut_usage_mc.py --sc-src 1 --mc-all-bimodal`

Build: `latexmk -pdf -interaction=nonstopmode -halt-on-error -auxdir=build -emulate-aux-dir valley_dst_report_en.tex`

(MC defaults to `--seed 0` unless specified).